

Finite element modeling of proximal femur with quantifiable weight-bearing area in standing position

Yang Peng

Guangzhou University of Chinese Medicine

Tian-Ye Lin

Guangzhou University of Chinese Medicine

Jing-Li Xu

Guangzhou University of Chinese Medicine

Hui-Yu Zeng

Guangzhou University of Chinese Medicine

Da Chen

Guangzhou University of Chinese Medicine

Bing-Lang Xiong

Guangzhou University of Chinese Medicine

Feng-Xiang Pang

Guangzhou University of Chinese Medicine

Zhen-Qiu Chen

Guangzhou University of Chinese Medicine

Wei He

Guangzhou University of Chinese Medicine

Qiu-Shi Wei

Guangzhou University of Chinese Medicine

Qing-Wen Zhang (✉ zh_qwen@163.com)

The First Affiliated Hospital of Guangzhou University of Chinese Medicine <https://orcid.org/0000-0002-5417-2970>

Research article

Keywords: Finite element modelling, Weight-bearing area, Image registration

Posted Date: January 6th, 2020

DOI: <https://doi.org/10.21203/rs.2.20068/v1>

License: © ⓘ This work is licensed under a Creative Commons Attribution 4.0 International License.

[Read Full License](#)

Abstract

Background

The positional distribution and size of the weight-bearing area of femoral head in the standing position as well as the direct active surface of joint force can directly affect the result of finite element (FE) stress analysis, however in most studies related separate FE models of femur, the division of this area is vague, imprecise and un-individualized. The purpose of this study was to quantify the positional distribution and size of the weight-bearing area of femoral head in standing position by a set of simple methods, to realize individualized reconstruction of proximal femur FE model.

Methods Five adult volunteers were recruited for X-ray and CT examination in the same simulated bipedal standing position with a specialized patented device. We extracted these image data, calculated the 2D weight-bearing area on X-ray image, reconstructed the 3D model of proximal femur based on CT data, and registered them to realize the 2D weight-bearing area to 3D transformation as the quantified weight-bearing surface. One of the 3D models of proximal femur was randomly selected for finite element analysis (FEA), and we defined three different loading surfaces, and compared their FEA results.

Results

A total of 10 weight-bearing surfaces in 5 volunteers were constructed, they were mainly distributed on the dome and anterolateral of femoral head with crescent shape, in the range of $1,218.63\text{mm}^2$ - $1,871.06\text{mm}^2$. The results of FEA showed stress magnitude and distribution in proximal femur FE models among three different loading conditions were significant differences, the loading case with quantized weight-bearing area was more in accordance with the physical phenomenon of the hip.

Conclusion

This study confirmed an effective FE modeling method of proximal femur, which can quantify weight-bearing area to define more reasonable load surface setting without increasing the actual modeling difficulty.

1. Background

FE technology plays an important role in digital orthopedic researches. Among them, as the largest weight-bearing joint in the human body, hip joint related FEA study has always been the research focus. At present, hip joint biomechanical researches are mainly based on gait-analysis based model or specific body movement posture model for mechanical analysis. To simplify the calculation process, researchers also use the static hip joint model in a single-legged standing posture as the research object, and analogize other motion states by specific linear proportional relations.

In our previous research, we established the standing hip model to perform mechanical research and recognized that in the standing position, the contact area as well as the weight-bearing area of femoral

head as the direct active surface of joint force, its positional distribution and size can directly affect the stress distribution of the femoral head[1]. There are lots of literature reports of mechanical analysis based on the separate FE model of femur, however most of them define weight-bearing area as ambiguous elliptical region, or load the joint force by simplifying the weight-bearing area into a point, which can affect the authenticity and accuracy of FEA. So, before a biomechanical FEA of the separate femoral head be carried out, it is necessary to define the weight-bearing area scientifically. Genda et al.[2] reported a method for calculating hip joint contact area in single-legged standing posture by X-ray film and verified its accuracy, but this method has not been applied to real case based FE model. We assume that there is the trade-off of easiness and accuracy between the full hip model and the simplified model. The purpose of this study is to explore the feasibility of using a set of simple methods to reconstruct the individualized proximal femur FE model with quantifiable weight-bearing area of femoral head in standing position, and provide a design idea of quantitative analysis for more accurate FE study.

2. Methods

2.1. Patients and Study Design

Five adult volunteers (2 males, 3 females, as shown in Tab. 1) without history of hip pain, lower limb disease or any other systemic diseases were recruited and subjects knew about the test scheme. X-ray and computerized tomography(CT) were conducted in all volunteers with the same position: simulated bipedal standing in supine position, bilateral anterior superior iliac spines at the same horizontal line, knees straight, patella up and heels together with the toes 30° apart. Anteroposterior (AP) view of pelvis (with a magnification marker): X-ray beam perpendicular to table, centered at the midpoint between the superior margin of the symphysis pubis and at the midpoint between the anterior superior iliac spines. CT scan (Aquilion 64, Toshiba Medical System Corp., Japan): 0.5mm slice thickness and 5mm interval, radiograph ranged from 1 cm above the highest point of iliac crest to 5 cm below the lesser trochanter. At above situation, a specialized patented device (National invention patent of China, NO. 201910159244.7, Fig. 1) was designed to ensure the same posture fixation while X-ray and CT were performed.

Table 1 Personal data and anatomical parameters of volunteers

Case No.	Age(y)/Sex	BMI(kg/m ²)	CE Angle Left/Right(°)
1	37/male	26.5	35/37
2	38/female	21.3	26/27
3	33/male	22.6	31/32
4	33/female	24.3	33/30
5	32/female	23.1	33/32

2.2. 3D reconstruction of proximal femur

CT image data were saved in DICOM format and imported into Mimics 16.0 software (Materialise Corp., Belgium) to reconstruct the 3D model of cortical bone and cancellous bone of proximal femur.

2.3. Establishment of 3D femoral head weight-bearing area based on 2D X-ray radiograph

The setting of the weight-bearing area was based on the specific anatomical parameters of the X-ray AP view of pelvis. Firstly, we calculated the magnification of the X-ray film by reference to standard marker (a coin) and restored the actual size, then identified 19 landmark points included the following (Fig.2): (1) point in the most lateral of greater trochanter (2) point in the top margin of greater trochanter (3) point in the most lateral of femoral head (4) point in the most lateral of acetabulum (5) point in the medial margin of sourcil line (6) point in the most medial of femoral head (7) point in the inferior margin of teardrop line (8) midpoint of the line connecting bilateral teardrop (9) point in the center of pubic symphysis (10) point in the inferior margin of ischium (11) point in the intersection between the posterior acetabular margin and inferior margin of femoral head (12) point in the most lateral of ilium (13) point in the inferior margin of ilium (14) point in the center of the fifth lumbar vertebrae (15) point in the inner margin of ilium nearest to the point 12 (16) point in the top margin of femoral head (17) point in the acetabular contour relative to point 16 (18) point in the lateral margin of teardrop relative to point 6 (19) center of femoral head. The calculation of anatomic parameters was referred to Genda et al., which based on the above landmark points: (a) Lateral margin of weight-bearing area (line 4-M): bisecting the angle 7-4-11 (b) Medial margin of weight-bearing area (line 5-W): connecting point 5 and W (midpoint between point 6 and 18).

2.4. Image registration of the proximal femur 3D reconstruction model and the 2D image of X-ray.

A datum plane parallel to the coronal plane of CT was established in Solidworks 2014 software (Dassault Systemes S.A., France) and extracted actual size 2D image of X-ray AP view of pelvis on this plane. View Adjustment of 3D reconstructed graphic of the proximal femur was taken based on X-ray 2D image as reference background to realize the registration of the 3D reconstructed graphic with 2D X-ray image in eliminate edge coloring mode by taking the specific anatomic markers of lesser trochanter and greater trochanter, femur contour as the registration points (Fig. 3). After satisfactory image registration, a datum plane α parallel to the perspective plane of the window was created.

2.5. Calculation of 3D weight-bearing area

Based on the registered image, the 2D landmark points on X-ray AP view of pelvis were transformed into the 3D points on the coordinate system of datum plane α by vertical projecting, and the line 4-M, line 5-W were recalculated on datum plane α . Then line 4-M and line 5-W trimmed surface α generating over the surface of femoral head with Offset Surface command (0mm) to become surface β . Referring to Genda et al.[2], we defined 30° below the horizontal plane through the center of the femoral head as inferior limit of the weight-bearing area, and thus trimmed surface β along the direction of joint reaction force to

generate surface γ , namely 3D weight-bearing area (Fig. 4). To facilitate post-processing of FEA, surface γ was filleted in 1mm.

Through above steps, a total of 10 weight-bearing surfaces and 10 proximal femur 3D models in 5 volunteers were constructed.

2.6. Finite element analysis

Mesh generation: One of the above proximal femur models was randomly selected and imported into Abaqus 6.14 software (Dassault Systemes S.A., France) to generate isotropic C3D10 tetrahedral elements with a mesh size of 2 mm. The total number of elements in the cortical bone mesh was 109,684 (210,154 nodes), the cancellous bone mesh was 69,566 (120,336 nodes).

Material Properties: The simplified model was defined by bi-material properties and material properties used for each component was referred to literature[3].

Boundary condition: A musculoskeletal multibody modeling framework in standing position was constructed by AnyBody Modeling System version 6.1 (AnyBody Technology, Denmark) and matched with the proximal femur 3D reconstruction model, then performed inverse dynamic loading and obtained the muscle and joint reaction force data (magnitude and direction) during standing and exported the data to the FE model for the boundary condition setting, as shown in Fig. 5. Constraints were applied to distal end of model, and all six degrees of freedom were constrained to zero.

Joint reaction force: To observe the effect of different joint reaction force areas on the internal stress distribution of femoral head, three different loading conditions were simulated, as shown in Fig. 6. In the first loading case A, joint reaction force was applied to weight-bearing area (surface γ) being established above. Two common joint reaction force loading methods in literature were designed as loading case B (circular region with diameter 2cm at the top of femoral head) and loading case C (apical point of femoral head), respectively. The joint reaction force simulating single-legged stance in three cases were loaded onto each corresponding coupling-surface of joint reaction force area. Meanwhile, a normal hemipelvis and entire hip joint (hemipelvis-hip) model which been established in our previous study[4] was introduced to compare with the models described above, and same load as ground reaction force was applied to the hemipelvis-hip model.

Defining path: To better analyze the internal stress change in femoral head, a path α was defined inside the model: from the vertex (node serial number: 2,716) to the head-neck junction (node serial number: 62,626) on Y-axis sagittal section (position serial number: -2.85069). 12 mesh elements were picked up on path α and recorded the stress values in principal stress orientation.

3. Results

3.1. Weight-bearing area distribution and size

In this study, a total of 10 weight-bearing surfaces in 5 volunteers were constructed through individualized process. The surfaces were mainly distributed on the dome and anterolateral of femoral head with crescent shape, as shown in Fig. 7. Quantifying the size: maximum area was 1,871.06 mm², minimum area was 1,218.63 mm². The results of literature comparison are shown in Tab. 2.

Table 2 The size and distribution of weight-bearing area with literature contrast.

literature	size	distribution
Wang[5]	1470 mm ² (acetabular)	dome of acetabular
Greenwald[6]	2002 mm ² (containing cartilage)	dome and anterolateral of femoral head
Brown[7]	1700 mm ²	dome and anterolateral of femoral head
Our study	1218.63-1871.06 mm ²	dome and anterolateral of femoral head

3.2. Stress magnitude and distribution

The results of FEA showed stress magnitude and distribution of proximal femur FE models in A, B and C three different loading conditions were significant differences. In loading case A with quantized weight-bearing area, the maximum stress (25.7MPa) of cortical bone located in the region of femoral neck-body junction, which was similar to that of hemipelvis-hip model (maximum stress was 24.04MPa), and different to that of loading case B and C, whose stress concentration appeared at the top region of femoral head (the maximum stress was 59.29MPa and 13.45MPa, respectively) where the joint reaction force applied to, as shown in Fig. 8. Analysis of internal stress distribution of femoral head. The stress values of 12 elements on path α in different loading conditions were extracted to plot the graph (Fig. 9), we discovered that stress patterns in loading case A and hemipelvis-hip model shared strong similarities, which was significantly different from loading case B and C. In loading case A, the internal stress concentration region loading principal stress reflected mechanical transfer path, whose region and sharp were consistent with the physiological distribution of compression trabeculae (Fig. 10), while this feature was not evident in either loading case B or C. Hence, the FEA results of loading case A with quantized weight-bearing area are more in accordance with the physical phenomenon of the hip.

4. Discussion

Abnormal biomechanical process is an important factor related to the development and progression of hip disease, FEA technology can be well used to study those mechanical characteristics and reveal the changing rules to guide treatment. Taking osteonecrosis of femoral head (ONFH) as an example, collapse is the most critical process in the four main pathological changes[8] (necrosis, repair, collapse and

osteoarthritis), previous studies have shown that the occurrence of collapse is the result of the interaction of biological and biomechanical factors[9]. In our prophase research, we have established the FE model of hemipelvis and entire hip joint containing necrosis[1], and expounded that one of mechanical mechanisms of collapse is the stress shielding effect leading to the uneven distribution of stress transmission in femoral head and the excessive concentration of stress on the surface (underlying subchondral bone) of the femoral head. And on this basis, we optimized focus debridement being used in fibular allograft with impaction bone grafting to treat ONFH. However, the conduction of stress in femoral head is actually affected by many factors, chief among them is the weight-bearing area of femoral head as the direct active surface of joint force in standing posture[6, 10]. In the research on FEA, the distribution and size of weight-bearing area can be well reflected by establishing a pelvis and entire hip joint model[11-14].

While, in the FE modeling approach of pelvis and entire hip joint, the numerical simulation of cartilage and complex algorithm defining for joint contact relationship need to be considered. These processes are tedious and time-consuming, which may increase the risk of subjective bias and diminish the validity of result, especially in the large sample test. For certain cases, researchers prefer constructing the separate FE model of femur (or proximal femur) to perform related mechanical analysis to improve the efficiency of FEA, which can be considered as a feasible alternative to simplify FE model of hip[15-18].

Different from the FE model of pelvis and entire hip joint, the region of joint reaction force as well as the weight-bearing area in such separate model with standing position needs to be defined before stress loading. Most of the related literature present to design weight-bearing area as an ambiguous elliptical region[19, 20], or load the joint force by simplifying it into a point[15, 21]. This can unify load condition and quickly realize the mechanical analysis. But in reality, weight-bearing area isn't nearly as elliptical or point. Kummer et al.[22] suggested that the weight-bearing area should be the overlap between the upper hemisphere of the femoral head and the acetabulum, known as the "spherical binangle". Daniel et al.[23] calculated by formula that the weight-bearing area should be in the area where the top of the femoral head overlaps with the acetabular cartilage surface, and can be affected by the shape of the acetabular cartilage surface. Greenwald et al.[6] through the experiment of 51 cadaveric specimens obtained the fan-shaped weight-bearing area in standing position distributing at the dome of femoral head. Bachtar et al. [24] also showed the crescent-shaped weight-bearing area at the superior and anterosuperior parts of the femoral head by the virtual FE simulation of hip with Gregory patch smoothing algorithm for contact elements. As shown in this research, we quantified the size and positional distribution of 10 weight-bearing areas of femoral head in standing position through individualized process, results of literature comparison confirm the reliability of study. The results of FEA demonstrate that the different of weight-bearing area leads to significant difference in stress distribution, the setting of FE model with quantized weight-bearing area is more in accordance with the physiological situation of the hip.

The calculation method of weight-bearing area of femoral head in standing position mainly refers to the theoretical formula proposed by Genda et al.[2], and the 3D reconstruction is realized by the principle of projection transformation and image registration. Ishimaru et al.[25] reported simulating X-ray by

projection transformation to create virtual radiographic image of 3D knee joint model and registering it with real X-ray film to realize visual reconstruction of polymer polyethylene patellar component and radiographically determine its external contour. Image registration is vital to the accurate construction of weight-bearing area in our modeling process, and obtaining X-ray, CT data of one volunteer in the same body posture is the premise of accurate registration. So, we designed a patented device to ensure the same posture fixation while X-ray and CT were performed.

The results of FEA show that the FE model of proximal femur with quantized weight-bearing area can successfully carry out force analysis and more in accordance with the physical phenomenon of the hip-femur. Compared with the traditional FE modeling method, the proposed method is more accurate and reasonable for the load surface setting without increasing the actual modeling difficulty. This research significance lies in that it established a quantifiable model basis for further exploring the biomechanical effects of changes in the weight-bearing area on the occurrence and development of femoral head-related diseases. Simultaneously it also provided a quantitative analysis design idea for more accurate FE research.

Our study has several limitations that warrant discussion. Even the assumption that using 2D X-ray film to determine 3D weight-bearing area still needs to be discussed. Through the 2D film alone, the shape and direction of the acetabulum cannot be accurately judged, thus ignoring its influence on the distribution of the weight-bearing area, which may lead to inaccuracy on the sagittal plane. Furthermore, the process of image registration mainly depended on manual work, so the accuracy of registration could be affected by subjective factor. Strictly, a true 3D FE model should be performed based on CT and MRI data including entire hip joint and pelvis to assure the reliability of the simulation. This study explored the feasibility of a more realistic and quantifiable simplified modeling method, which can particularly be applied for rapid and individual modeling of large sample. However, further works are required to consider the correlation and translation between X-ray and CT images in the shape and direction of acetabular, which will be based on sufficient clinical research data. And automatic image registration will be considered to reduce subjective bias by means of coordinate point registration.

5. Conclusion

This study confirmed an effective FE modeling method of proximal femur, which can quantify weight-bearing area to define more reasonable load surface setting without increasing the actual modeling difficulty, those researches which involve the FEA of the femoral side could benefit.

Abbreviations

FE:Finite element;FEA:finite element analysis;CT:computerized tomography; AP:Anteroposterior

Declarations

The authors would like to thank Wang Haibin in Guangzhou University of Traditional Chinese Medicine and Chen LeiLei in Guangzhou University of Traditional Chinese Medicine for help with picture making and English polishing.

Authors' contributions

YP and LTY were involved in data analysis and manuscript writing. XJL, ZHY, XBL, CD, CZQ, and PFX were involved in data analysis. HW was involved in statistical analysis. WQS was involved in manuscript editing. ZQW was involved in materials processing. All authors have read and approved the manuscript and ensure that this is the case.

Funding

This study was supported by grants from the National Natural Science Foundation of China (Grant No. 81873327), Natural Science Foundation of Guangdong (Grant No. 2015A030313353), Scientific Research Project of Chinese Medicine of Guangdong (Grant No. 20191116) and Excellent Doctoral Dissertation Incubation Grant of First Clinical School of Guangzhou University of Chinese Medicine (Grant No. YB201802). The funders had no role in study design, data collection and analysis, decision to publish, nor in writing the manuscript.

Availability of data and materials

All data and materials are contained within the manuscript

Ethics approval and consent to participate

This study was conducted in agreement with the Declaration of Helsinki and its later amendments or comparable ethical standards and had been approved by the ethics board of The First Affiliated Hospital of Guangzhou University of Chinese Medicine (No: Y2019118).

Consent for publication

Not applicable.

Competing interests

The authors declare no conflict of interest.

References

[1] G.Q. Zhou, Z.H. Pang, Q.Q. Chen, W. He, Z.Q. Chen, L.L. Chen, Z.Q. Li, Reconstruction of the biomechanical transfer path of femoral head necrosis: a subject-specific finite element investigation, *Comput Biol Med*, 52 (2014) 96-101. <https://doi.org/10.1016/j.combiomed.2014.04.002>

- [2] E. Genda, N. Iwasaki, G. Li, B.A. MacWilliams, P.J. Barrance, E.Y. Chao, Normal hip joint contact pressure distribution in single-leg standing—effect of gender and anatomic parameters, *J Biomech*, 34 (2001) 895-905.[https://doi.org/10.1016/S0021-9290\(01\)00041-0](https://doi.org/10.1016/S0021-9290(01)00041-0)
- [3] D. Grecu, I. Puculev, M. Negru, D.N. Tarnita, N. Ionovici, R. Dita, Numerical simulations of the 3D virtual model of the human hip joint, using finite element method, *Rom J Morphol Embryol*, 51 (2010) 151-155.
- [4] P. Yang, Q.S. Wei, Z.Q. Chen, D. Wang, D. Chen, W. He, Q.W. Zhang, Construction of finite element models of hemipelvis and total hip joint using multi-modality image registration technique, *J Trad Chin Orthop Trauma*, 29 (2017) 1-6.
- [5] G. Wang, W. Huang, Q. Song, J. Liang, Three-dimensional finite analysis of acetabular contact pressure and contact area during normal walking, *Asian J Surg*, 40 (2017) 463-469.<https://doi.org/10.1016/j.asjsur.2016.07.002>
- [6] A.S. Greenwald, D.W. Haynes, Weight-bearing areas in the human hip joint, *J Bone Joint Surg Br*, 54 (1972) 157-163. <https://doi.org/10.1302/0301-620x.54b1.157>
- [7] T.D. Brown, D.T. Shaw, In vitro contact stress distributions in the natural human hip, *J Biomech*, 16 (1983) 373-384.[https://doi.org/10.1016/0021-9290\(83\)90071-4](https://doi.org/10.1016/0021-9290(83)90071-4)
- [8] Q. Zhang, F. Yang, Y. Chen, H. Wang, D. Chen, W. He, P. Chen, Chinese herbal medicine formulas as adjuvant therapy for osteonecrosis of the femoral head: A systematic review and meta-analysis of randomized controlled trials, *Medicine*, 97 (2018).<https://doi.org/10.1097/md.00000000000012196>
- [9] W.L. Gou, Q. Lu, X. Wang, Y. Wang, J. Peng, S.B. Lu, Key pathway to prevent the collapse of femoral head in osteonecrosis, *Eur Rev Med Pharmacol Sci*, 19 (2015) 2766-2774.
- [10] A. Iglic, V. Kralj-Iglic, M. Daniel, A. Macek-Lebar, Computer determination of contact stress distribution and size of weight bearing area in the human hip joint, *Comput Methods Biomech Biomed Engin*, 5 (2002) 185-192.<https://doi.org/10.1080/10255840290010300>
- [11] M. Wang, L. Wang, P. Li, Y. Fu, A novel modelling and simulation method of hip joint surface contact stress, *Bioengineered*, 8 (2017) 105-112.<https://doi.org/10.1080/21655979.2016.1227630>
- [12] H. Yoshida, A. Faust, J. Wilckens, M. Kitagawa, J. Fetto, E.Y. Chao, Three-dimensional dynamic hip contact area and pressure distribution during activities of daily living, *J Biomech*, 39 (2006) 1996-2004.<https://doi.org/10.1016/j.jbiomech.2005.06.026>
- [13] M. Noda, Y. Nakamura, K. Adachi, Y. Saegusa, M. Takahashi, Dynamic finite element analysis of implants for femoral neck fractures simulating walking, *J Orthop Surg (Hong Kong)*, 26 (2018) 2309499018777899.<https://doi.org/10.1177/2309499018777899>

- [14] K. Akiyama, T. Sakai, J. Koyanagi, H. Yoshikawa, K. Sugamoto, In vivo hip joint contact distribution and bony impingement in normal and dysplastic human hips, *J Orthop Res*, 31 (2013) 1611-1619. <https://doi.org/10.1002/jor.22414>
- [15] Z. Chen, Y. Xu, Z. Qi, J. Zho, The formation and function of the sclerosis rim in the femoral head: A biomechanical point of view, *Med Eng Phys*, 37 (2015) 1125-1132. <https://doi.org/10.1016/j.medengphy.2015.09.005>
- [16] A. Furui, N. Terada, K. Mito, Mechanical simulation study of postoperative displacement of trochanteric fractures using the finite element method, *J Orthop Surg (Hong Kong)*, 13 (2018) 300. <https://doi.org/10.1186/s13018-018-1011-y>
- [17] K. Gok, S. Inal, A. Gok, E. Gulbandilar, Comparison of effects of different screw materials in the triangle fixation of femoral neck fractures, *J Mater Sci Mater Med*, 28 (2017) 81. <https://doi.org/10.1007/s10856-017-5890-y>
- [18] H. Ziaeiipoor, M. Taylor, M. Pandy, S. Martelli, A novel training-free method for real-time prediction of femoral strain, *J Biomech*, 86 (2019) 110-116. <https://doi.org/10.1016/j.jbiomech.2019.01.057>
- [19] Y. Kawabata, K. Matsuo, Y. Nezu, T. Kamiishi, Y. Inaba, T. Saito, The risk assessment of pathological fracture in the proximal femur using a CT-based finite element method, *J ORTHOP SCI*, 22 (2017) 931-937. <https://doi.org/10.1016/j.jos.2017.05.015>
- [20] T. Yu, L. Xie, F. Chu, A sclerotic rim provides mechanical support for the femoral head in osteonecrosis, *Orthopedics*, 38 (2015) e374-379. <https://doi.org/10.3928/01477447-20150504-53>
- [21] J. Li, M. Wang, L. Li, H. Zhang, M. Hao, C. Li, L. Han, J. Zhou, K. Wang, Finite element analysis of different configurations of fully threaded cannulated screw in the treatment of unstable femoral neck fractures, *J Orthop Surg Res*, 13 (2018) 272. <https://doi.org/10.1186/s13018-018-0970-3>
- [22] B. Kummer, Biomechanics of the hip and knee joint, *Engineering in Medicine*, Springer 1976, pp. 24-52. https://doi.org/10.1007/978-3-642-66369-7_2
- [23] M. Daniel, A. Iglic, V. Kralj-Iglic, The shape of acetabular cartilage optimizes hip contact stress distribution, *J Anat*, 207 (2005) 85-91. <https://doi.org/10.1111/j.1469-7580.2005.00425.x>
- [24] F. Bachtar, X. Chen, T. Hisada, Finite element contact analysis of the hip joint, *Med Biol Eng Comput*, 44 (2006) 643-651.
- [25] M. Ishimaru, Y. Shiraishi, S. Ikebe, H. Higaki, K. Hino, Y. Onishi, H. Miura, Three-dimensional motion analysis of the patellar component in total knee arthroplasty by the image matching method using image correlations, *J ORTHOP RES*, 32 (2014) 619-626. <https://doi.org/10.1002/jor.22596>

Figures



Figure 1

A specialized patented device designed to ensure the same posture fixation while X-ray and CT were performed.

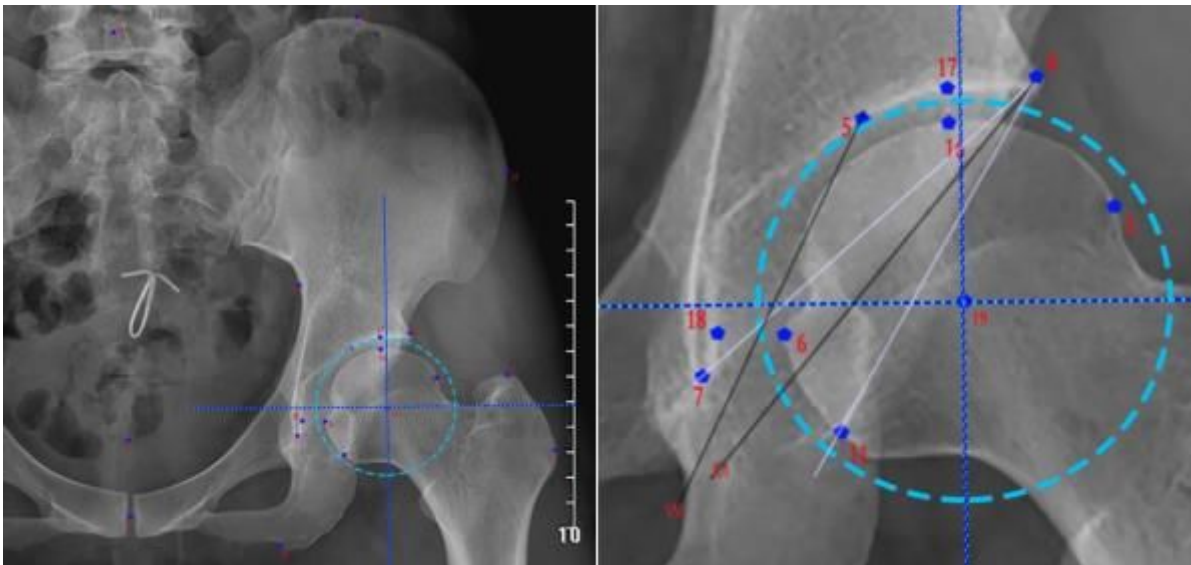


Figure 2

Identification of the anatomical landmarks on the AP radiograph to define the inner and outer edge of weight-bearing area

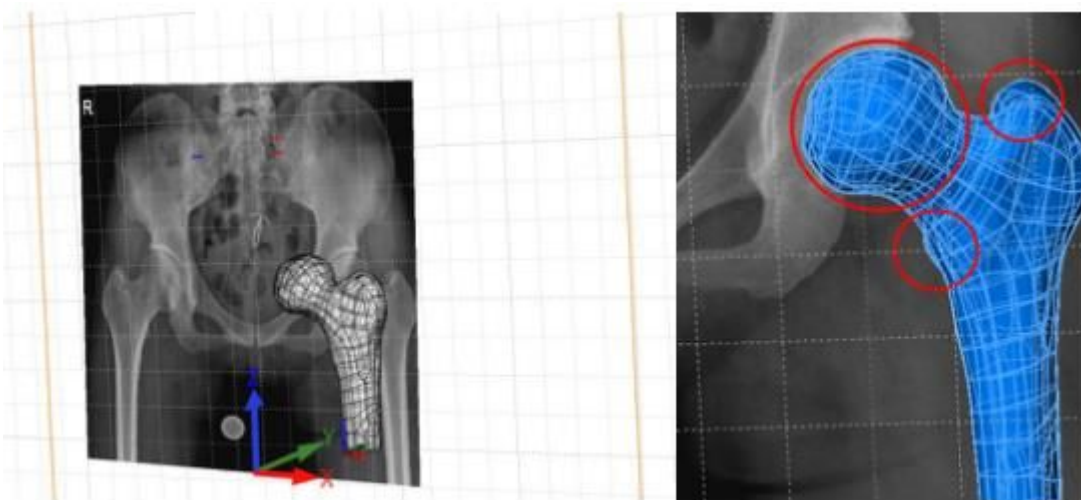


Figure 3

Registration of the proximal femur 3D model and X-ray image based on greater trochanter, lesser trochanter and femur contour

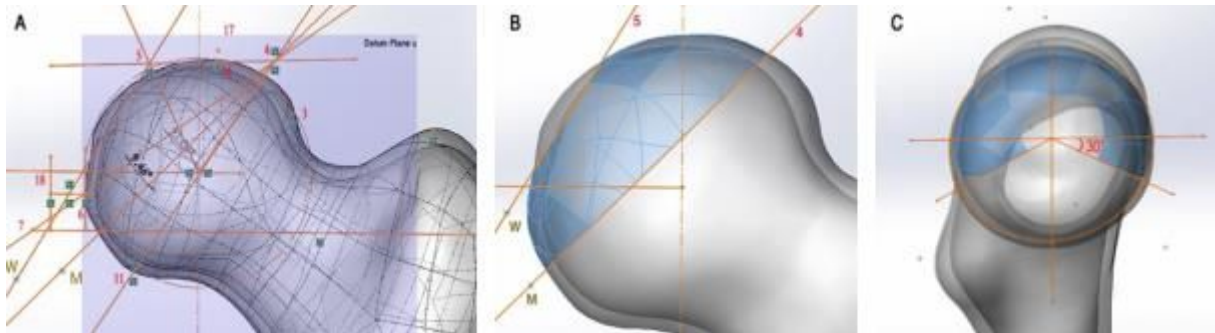


Figure 4

Calculation of 3D weight-bearing area. A: transformation of the landmarks from X-Ray image to the datum plane α ; B, C: definition of the limit line to trim out the shape of weight-bearing surface

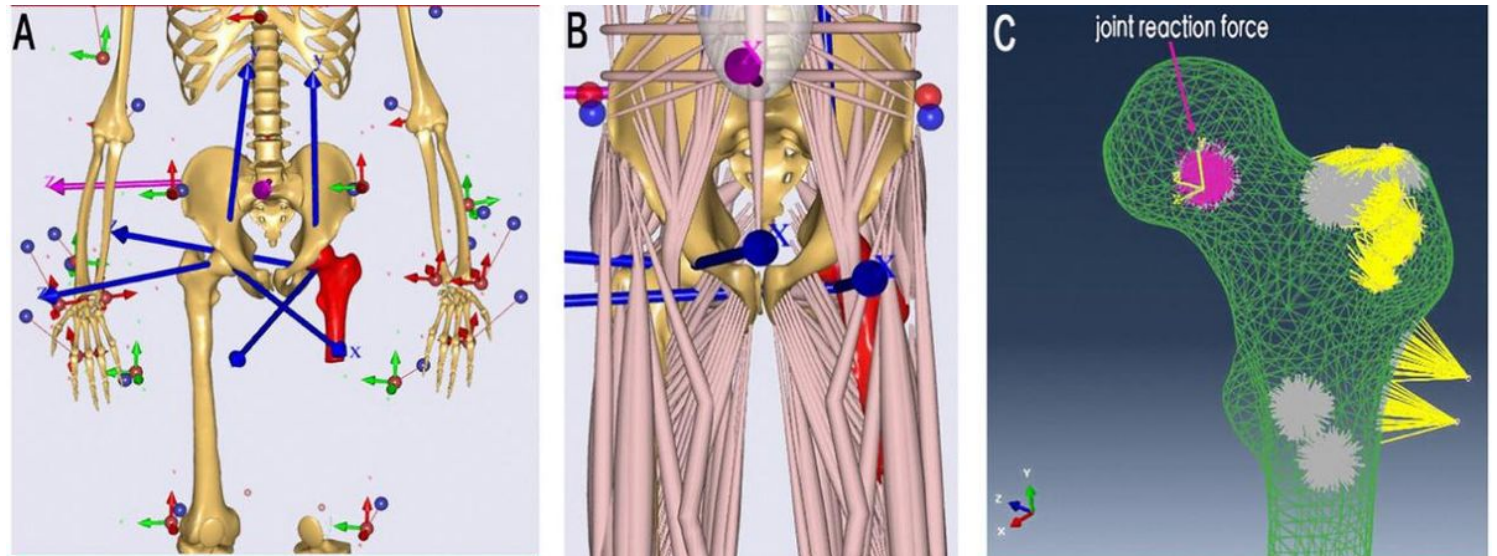


Figure 5

Muscle and joint reaction force. A, B: musculoskeletal multibody modeling framework (before and after inverse dynamics loading) matched with the proximal femur model; C: muscle and joint reaction force was applied to FE model.

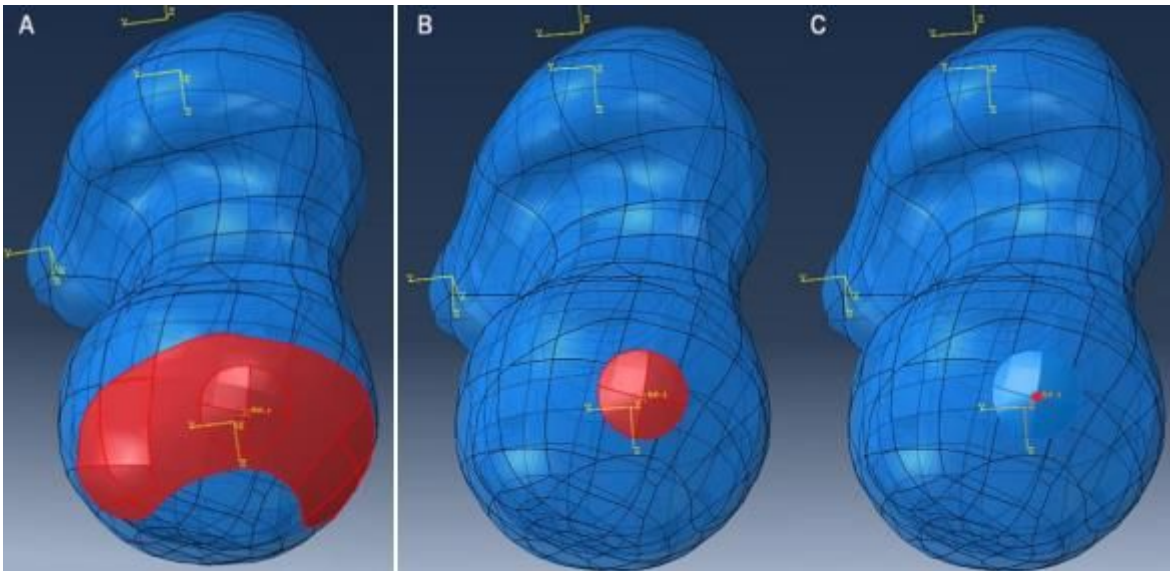


Figure 6

Models with different loading conditions

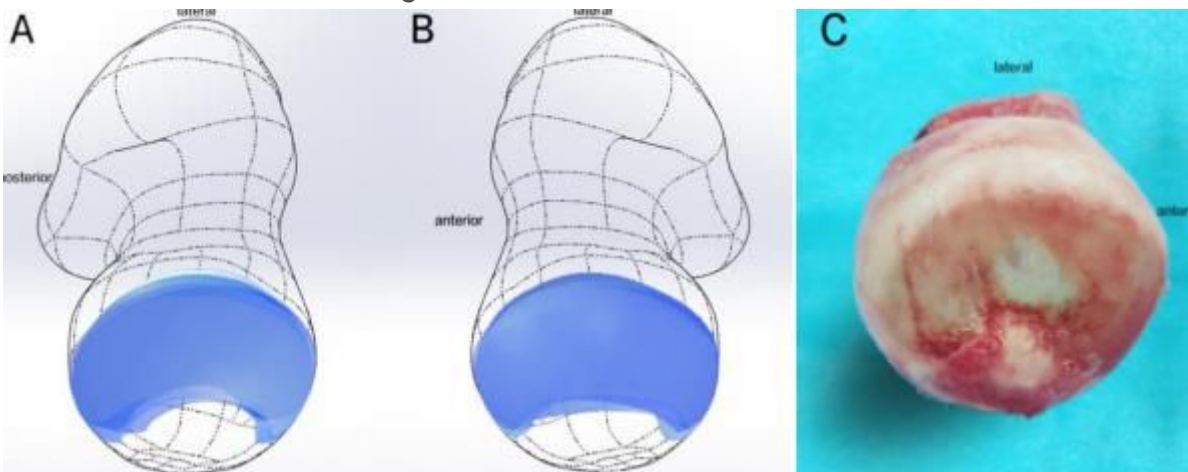


Figure 7

Distribution of weight-bearing area on the femoral head surface. A: left side in 5 volunteers; B: right side in 5 volunteers; C: a femoral head of arthritis patient removed in joint replacement surgery with obvious cartilage wear in weight-bearing area.

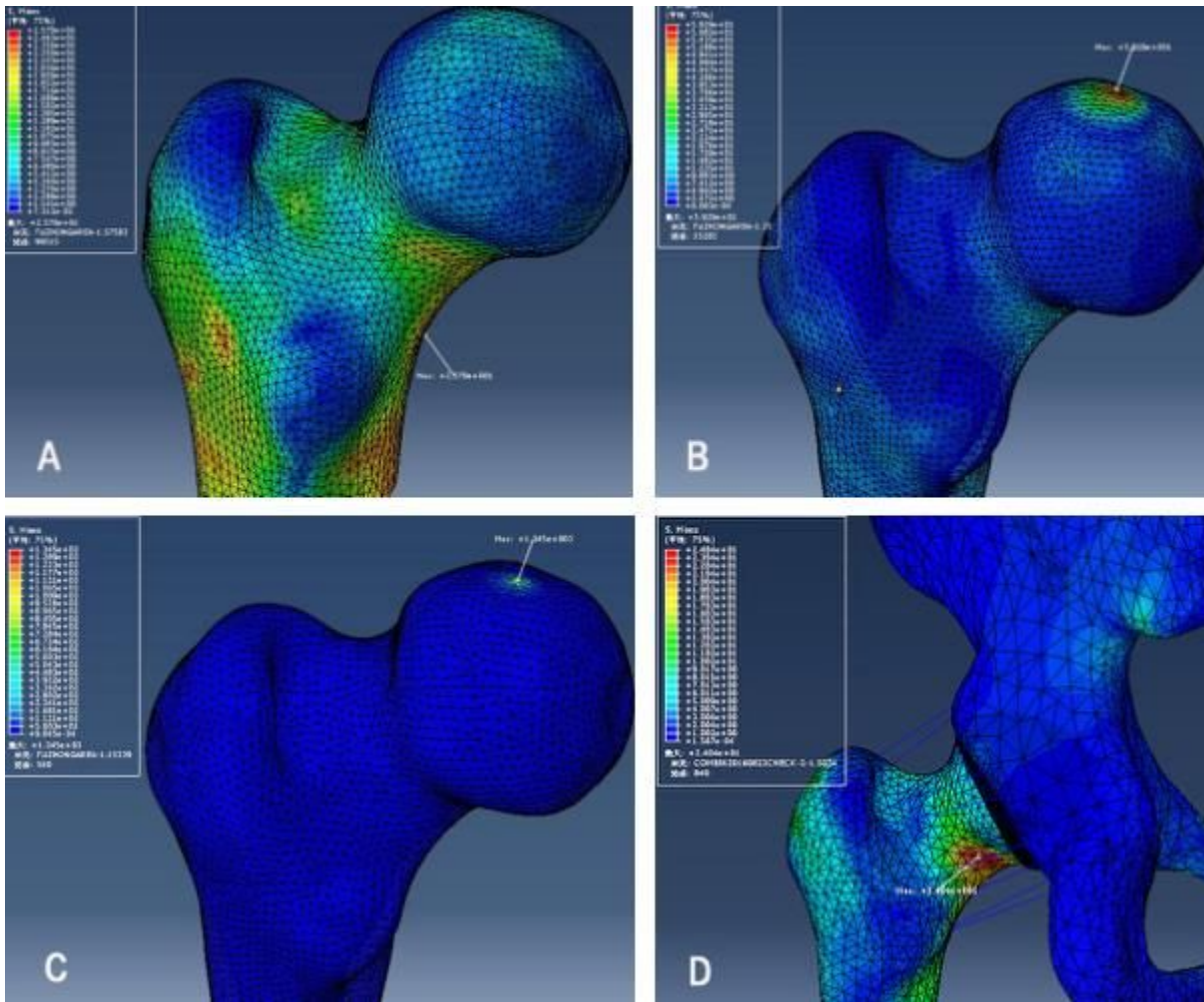


Figure 8

The distribution of maximum Von Mises stress in femoral cortical bone. A, B and C: models in loading case A, B and C; D: hemipelvis-hip model.

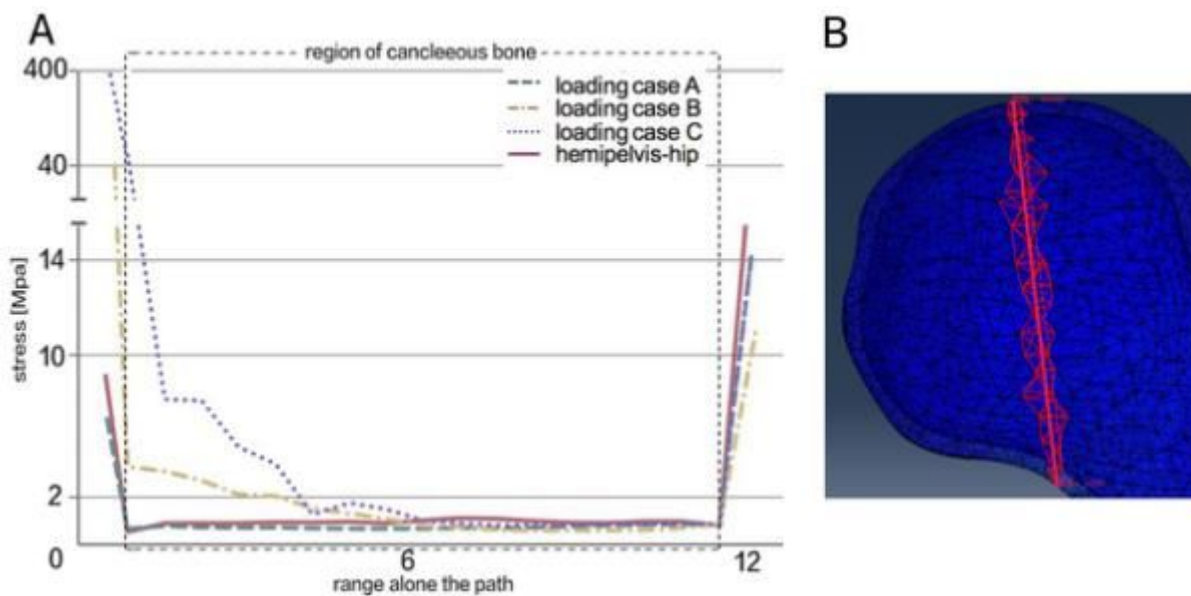


Figure 9

Comparison of principle stress changes in different loading conditions on path α . A: stress magnitude and distribution in proximal femur FE models among three different loading conditions were significant differences ($p < 0.05$), the loading case A (quantized weight-bearing area) was more in accordance with the hemipelvis-hip model; B: definition of path α .

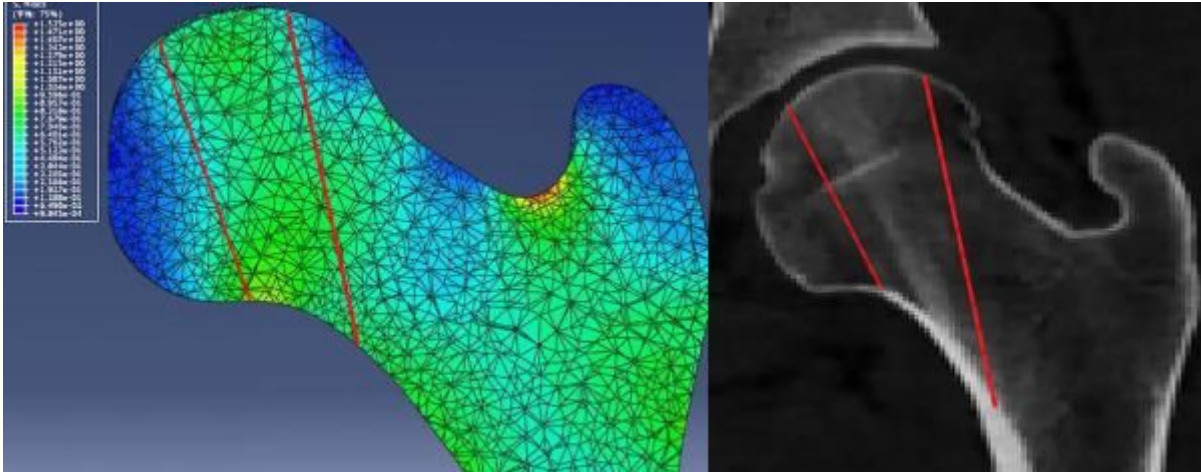


Figure 10

Stress cloud chart showed a stress concentration area appeared in femoral head, that was coherent with the stress bone trabecula located in femoral head.